NOTE

Thrust force characterization of free-swimming soft robotic jellyfish

To cite this article: Jennifer Frame et al 2018 Bioinspir. Biomim. 13 064001

View the <u>article online</u> for updates and enhancements.



IOP ebooks™

Bringing you innovative digital publishing with leading voices to create your essential collection of books in STEM research.

Start exploring the collection - download the first chapter of every title for free.

Bioinspiration & Biomimetics



RECEIVED 27 April 2018

DEVICED

10 August 2018

ACCEPTED FOR PUBLICATION 24 August 2018

PUBLISHED 18 September 2018 NOTE

Thrust force characterization of free-swimming soft robotic jellyfish

Jennifer Frame¹, Nick Lopez², Oscar Curet² and Erik D Engeberg^{2,3,4,5,6}

- ¹ Naval Surface Warfare Center Carderock Division, 9500 MacArthur Blvd, Bethesda, MD 20817, United States of America
- ² Department of Ocean and Mechanical Engineering, Florida Atlantic University, Boca Raton, FL 33431, United States of America
- ³ Center for Complex Systems and Brain Science, Florida Atlantic University, Boca Raton, FL 33431, United States of America
- ⁴ Associate Faculty: Center for Complex Systems and Brain Sciences, Ocean and Mechanical Engineering Department, Florida Atlantic University, 777 Glades Rd, Bldg. 36; Room 178, Boca Raton, FL 33431, United States of America
- ⁵ Author to whom any correspondence should be addressed.
- 6 http://biorobotics.fau.edu/

E-mail: eengeberg@fau.edu

Keywords: soft robotics, jellyfish, underwater vehicle

Supplementary material for this article is available online

Abstract

Five unique soft robotic jellyfish were manufactured with eight pneumatic network tentacle actuators extending radially from their centers. These jellyfish robots were able to freely swim untethered in the ocean, to steer from side to side, and to swim through orifices more narrow than the nominal diameter of the jellyfish. Each of the five jellyfish robots were manufactured with a different composition of body and tentacle actuator Shore hardness. A three-factor study was performed with these five jellyfish robots to determine the impact that actuator material Shore hardness, actuation frequency, and tentacle stroke actuation amplitude had upon the measured thrust force. It was found that all three of these factors significantly impacted mean thrust force generation, which peaked with a half-stroke actuation amplitude at a frequency of 0.8 Hz.

1. Introduction

Soft robots have tremendous potential to explore and monitor delicate marine ecosystems like coral reefs without causing unintentional damage to fragile objects [1, 2]. This is one reason that development of biomimetic soft robotic fish and marine animals have been steadily gaining popularity within the research community in recent years [3–5]. Many different aquatic animals have provided inspiration for novel robot design features, including the octopus [6–8], turtle [9], knifefish [10], manta ray [11], and jellyfish [12].

Among these, jellyfish have been classified as highly efficient swimmers [13, 14], so they are an excellent candidate for underwater robot design inspiration. Jellyfish propulsive performance is linked to the shape of the body, or bell, which can produce a combination of vortex [15, 16], jet propulsion [17], rowing [18], and suction-based locomotion [19]. Jellyfish can also turn via an asymmetric contraction of the body, which can lead to purposefully oriented directional swimming based on cues in the water column [20] and from visual stimuli [21, 22].

Prior designs of robotic jellyfish have used a variety of different classes of actuators to mimic the shape and motion of common jellyfish species such as the *A. victoria* and *A. aurita*. Six-bar linkage mechanisms have been used to drive a miniature jellyfish robot with four tentacles [23]. Shape memory alloy actuators that were heated electrically [12, 24] or by hydrogen fuel [25] have been used for robotic jellyfish propulsors, as have ionic polymer metal composites [26, 27] and dielectric elastomers [28]. Other implementations of robotic jellyfish have been controlled by electromagnetic actuation systems [29], iris mechanisms [30], tension springs [31], and bioengineered tissue [32].

In contrast, this paper presents the design, fabrication, and control of unique, free-swimming soft robotic jellyfish actuated by hydraulic networks (figure 1) [33]. These jellyfish robots can swim untethered in the ocean, squeeze through orifices more narrow than the nominal diameter of the jellyfish, and steer from side to side. Preliminary work with this jellyfish robot has been presented at conferences [34, 35]. This paper presents substantial contributions over these prior conference publications through a three factor study on the impact that the jellyfish material composition,



Figure 1. (a) and (b) The jellyfish robot swimming vertically in the Atlantic Ocean. (c) Live jellyfish in ephyra stage of life cycle. (d) Free swimming robotic jellyfish in the EroJacks Reef (e) four of the jellyfish robots swimming in the ocean.

actuation frequency, and actuation stroke amplitude had upon the thrust force generated by five different jellyfish robots. Furthermore, the ability to swim through orifices is also newly demonstrated.

2. Soft jellyfish robot design and manufacturing

2.1. Design considerations

The use of eight actuators radially extending from the center of the jellyfish (figure 1) is similar to the form of a moon jellyfish (Aurelia aurita) during the ephyra stage of its life cycle (figure 1(c)), before becoming a fully grown medusa. One main application of the jellyfish robot is for exploring and monitoring delicate ecosystems, so soft hydraulic network actuators were chosen due to their inherent potential to minimize inadvertent damage to fragile biological systems [1, 36]. Live jellyfish essentially have neutral buoyancy, so water was chosen as the medium to inflate the hydraulic network actuators while freely swimming in the ocean, pool, or aquarium. One issue that can occur with hydraulic or pneumatic networks is that the individual chambers farthest from the pump can bulge disproportionately. This problem was mitigated through design of oblong shaped tentacles conceptually similar to the form factor of the finger actuators shown in [36].

To enable the jellyfish to steer, two impeller pumps were used to inflate the eight tentacles, four tentacles per pump on opposing sides of the robot. The impeller pump design produced an open circuit of water flow, where water from the environment was pumped into the soft actuators to produce a swimming stroke. When the pumps were not powered, the elasticity of the tentacle actuator silicon rubber material (Ecoflex, Smooth-On, Inc., Macungie, USA) would con-

strict the actuators to exhaust the water back into the environment during the relaxation phase of the locomotion cycle. Use of inherent elasticity in the return motion is similar to the passive elasticity demonstrated by live jellyfish after bell contractions [37] and parallels natural jellyfish kinematics where changes in bell volume are crucial during locomotion [38]. This design also removed need for valves, thus reducing control complexity, space requirements, and cost. Additionally, the open circuit of water flow between the robot and environment is more efficient than a design that has a closed circuit of water flow with all water internally stored within the jellyfish. This kind of closed circuit design would require a larger internal reservoir purely for storing water to inflate the tentacle actuators, increasing drag and mass. While the open circuit flow of water is not exactly the same as live jellyfish, it is practical from a robotic design standpoint. Thus, an open circuit flow of water between the jellyfish and the environment was selected.

2.2. Jellyfish robot fabrication

Mold models for the jellyfish robot were designed in SolidWorks and subsequently 3D printed with an Ultimaker 2 out of PLA (figures 2(a) and (b)). Each tentacle had a common channel extending radially outward from the center of the robot; four of these channels were connected on each side of the jellyfish so that four tentacles could be driven by a single impeller pump (figure 2(c)). Two pumps were used to actuate the eight tentacles, four tentacles per pump. The external structure of the actuators are shown in figure 2(d) which have internal geometry shown in figures 2(c) and (e).

Next, the molds were sprayed with a release agent (Ease Release 200) and allowed to dry for 20 min. The

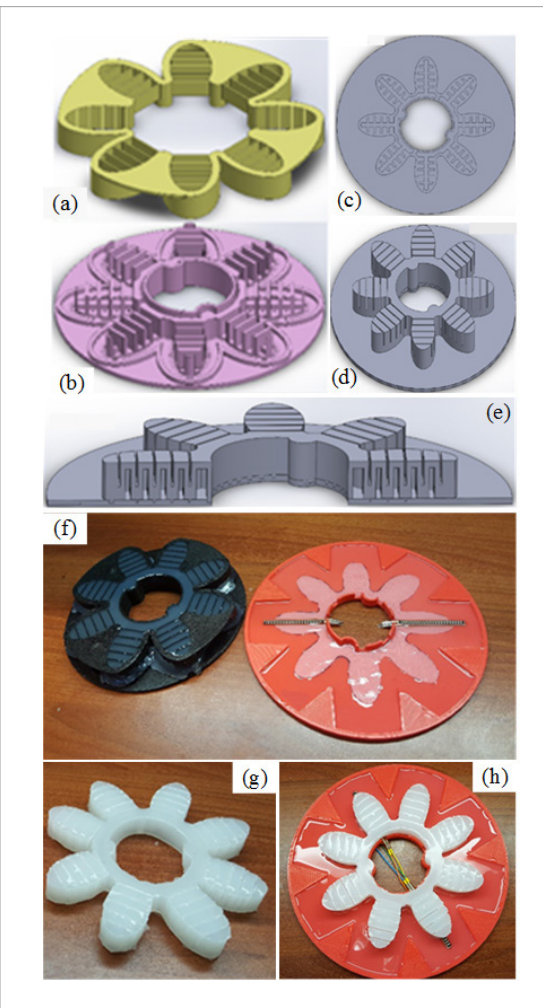


Figure 2. (a) Top and (b) bottom tentacle actuator molds were 3D printed. (c) Top view shows common actuator channels. (d) Isometric and (e) side-cut views of the soft actuators. (f) The tentacle actuators and segmented flap molds were filled with silicon rubber. Flexible resistive sensors were integrated to measure the angular posture of each half of the jellyfish. (g) Cured jellyfish robot tentacle actuators. (h) The tentacles bond to the flap.

silicon rubber (Ecoflex) was measured, and mixed with a 1:1 ratio, de-gassed for 5 min, and poured into the molds. The top (figure 2(a)) and bottom (figure 2(b)) molds for the tentacle actuators were mated and filled with silicon rubber (figure 2(f), left)). Another 3D printed mold for the jellyfish flap was coated with a thin layer of degassed silicon rubber (figure 2(f), right)). Polyester was used to provide reinforcement at the base of the actuators, which added mechanical strength to prevent ruptures and bulges. A stencil was made to trace the actuator pattern onto the polyester fabric which was trimmed with scissors. The polyester actuator reinforcement was placed over this layer on the flap and additional silicon rubber was poured atop the spots where position sensors were to be added. Flexible resistive sensors were placed on top of this extra silicon rubber to enable the jellyfish to sense the curvature of the actuators. Finally, another thin layer of silicon rubber was poured over the sensors to embed them within the flap (figure 2(f), right).

The silicon rubber comprising the tentacle actuators was allowed to cure for 24h and then carefully removed from the molds (figure 2(g)). Next, the top of the flap was thinly coated with 20 ml of silicon rubber and the demolded actuators were carefully placed atop the actuator layer of polyester fabric reinforcement (figure 2(h)). Another 24h were allowed to enable the actuators to bond securely to the flap. The tip-to-tip length of the jellyfish tentacle actuators was 160 mm and the maximum diameter of the jellyfish flap was 210 mm.

A cylindrical housing for the jellyfish microcontroller and electronics was 3D printed out of ABS with an Axiom AirWolf. A Teensy USB development board was used to control the jellyfish and printed circuit boards (PCBs) were designed for the electronics and sensors. Each Teensy 3.2 was mounted on a 45.7 mm × 22.9 mm PCB which was outfitted with an Invensense MPU-9250 9 axis motion sensor, and a 16 MB Flash memory chip (figure 3(a)). 24 gauge wires were used to connect a water temperature sensor (MCP9701A) and the two 55.9 mm flexible resistors (FS-L-0112-103-ST, Spectra Symbol, Salt Lake City, USA) that were imbedded in the jellyfish body to the PCB. Sensor and pump wires entered the housing from small holes in the bottom of the canister, which were sealed afterwards with silicone RTV. After this silicone dried for 24 h, epoxy was then poured into the bottom of the canister to ensure the through-holes were water-

Two submersible impeller pumps (Fafada) were chosen to actuate the two sides of the jellyfish: four tentacles per pump. These submersible 3 V DC motor mini pumps are rated for a maximum flow rate of 120 l h⁻¹. The impeller pumps were mounted onto the underside of the central canister of the robot jellyfish and flexible rubber tubes were connected between the pump outlets and the inlet to each hydraulic network of four tentacles on each half of the robot (figure 3(b)). The exhaust ports of the pumps were vertically aligned with the canister so that water would be exhausted directly downward if the jellyfish were swimming upward.

Two Allegro Microsystems, Inc. Hall effect sensors (A3212EUA-T) were mounted on the motherboard as a way to magnetically communicate with the robotic jellyfish without having to open the electronics housing. This enabled operators to simply cycle through jellyfish operational modes with a magnet while underwater without opening the electronics housing. Three LEDs were placed on the PCB to visually provide operational state feedback to the operator.

After installing all wires and sensors within the canister (figure 3(c)), an O-ring was situated in a groove on the top of the electronics canister and the lid was screwed into place. The IMU and temperature sensors, while not used for the present study, will afford the jellyfish robot an ability to sense itself and the environment in future works.

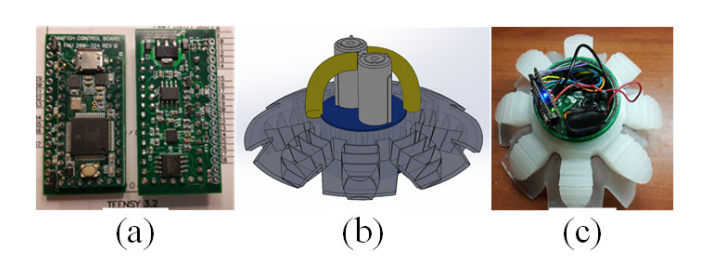


Figure 3. (a) PCB to control the soft robotic jellyfish. (b) Mounting of pumps onto the underside of the jellyfish robot central canister. Flexible rubber tubes were connected between the pump outlets and the inlet to both sets of four hydraulic tentacle actuators. (c) Integration of electronics within the central canister housing.

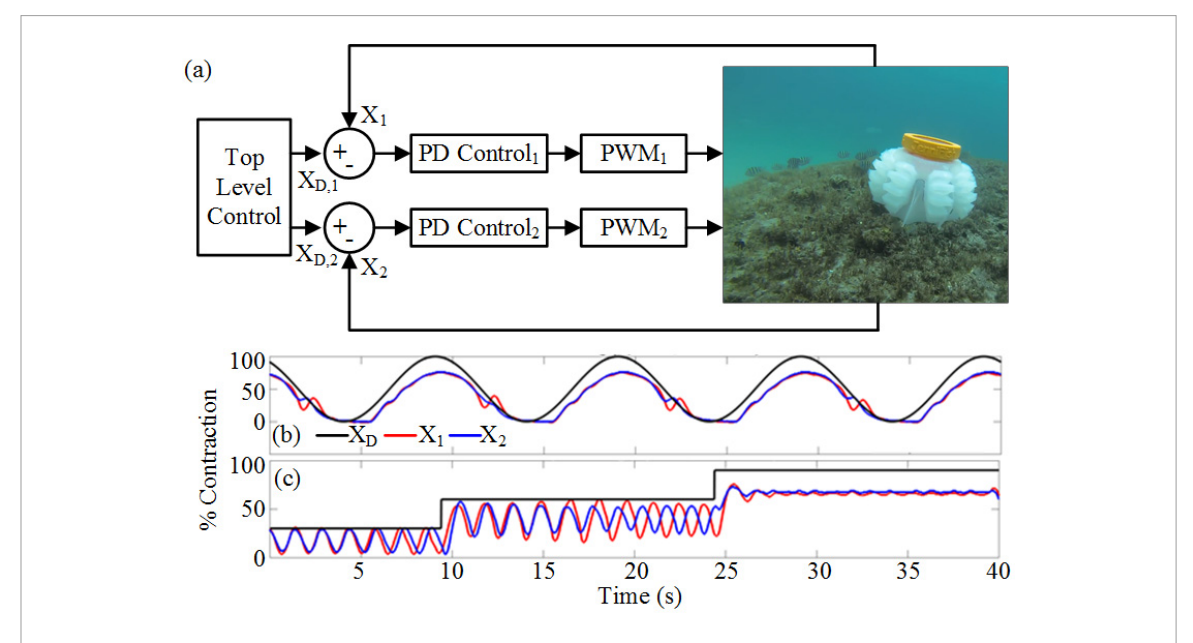


Figure 4. (a) PD controllers were programmed in Arduino for each pump to control four tentacles on each half of the jellyfish using angular position feedback from the embedded flexible sensors. (b) Sine wave tracking was only possible with a low frequency without eliciting oscillatory dynamics. (c) The step response revealed the highly underdamped system dynamics.

3. Experimental methods

3.1. Jellyfish tentacle controllers to investigate natural frequency

Proportional derivative (PD) controllers were coded in Arduino to control the angular posture of both sides of the jellyfish robot (X_1 and X_2) using feedback from the corresponding flexible resistive sensors (figure 4(a)) that were embedded in tentacles on each side of the jellyfish (figure 2(f)). The purpose of these experiments was to discover the natural frequency of the jellyfish actuation system for comparison to the thrust force measurement experiments described subsequently. The top level controller coordinated the desired postures of both sets of tentacles. Both sinusoidal tracking and step response experiments were performed to better understand the capabilities and dynamics of the jellyfish robot. The step response experiments were conducted with three different tentacle actuation amplitudes. In these experiments, the desired angular posture of the tentacles ($X_{D,1}$ and $X_{D,2}$, respectively) were made equal $(X_{D,1} = X_{D,2})$ so both sides of the jellyfish would move in unison. As will be subsequently shown, the step response of the system

revealed nearly undamped system dynamics while under position control.

3.2. Thrust force measurements

The impact that three different independent variables had upon the measured thrust force were investigated in this study: jellyfish material Shore hardness, actuation stroke amplitude, and actuation frequency. Five different material Shore hardness compositions of tentacle actuator and flap materials were considered, which necessitated the fabrication of five different jellyfish robots from silicon rubber using the process described in section 2.2. For each of these five jellyfish robots, full stroke and half stroke tentacle actuation amplitudes were explored, both of which were evaluated with ten actuation frequencies ranging from 0.1 Hz to 1 Hz with 0.1 Hz increments. A full stroke went from the relaxed pose to a fully contracted pose similar to that shown in figures 5(b)-(d), while a half stroke went from a halfway contracted to a fully contracted posture similar to the sequence shown in figures 6(b)-(d). The five different jellyfish robots had actuator-flap material Shore hardness compositions of 30-10, 30-20, 30–30, 30–50, and 50–50 (figure 7, top-left inset).

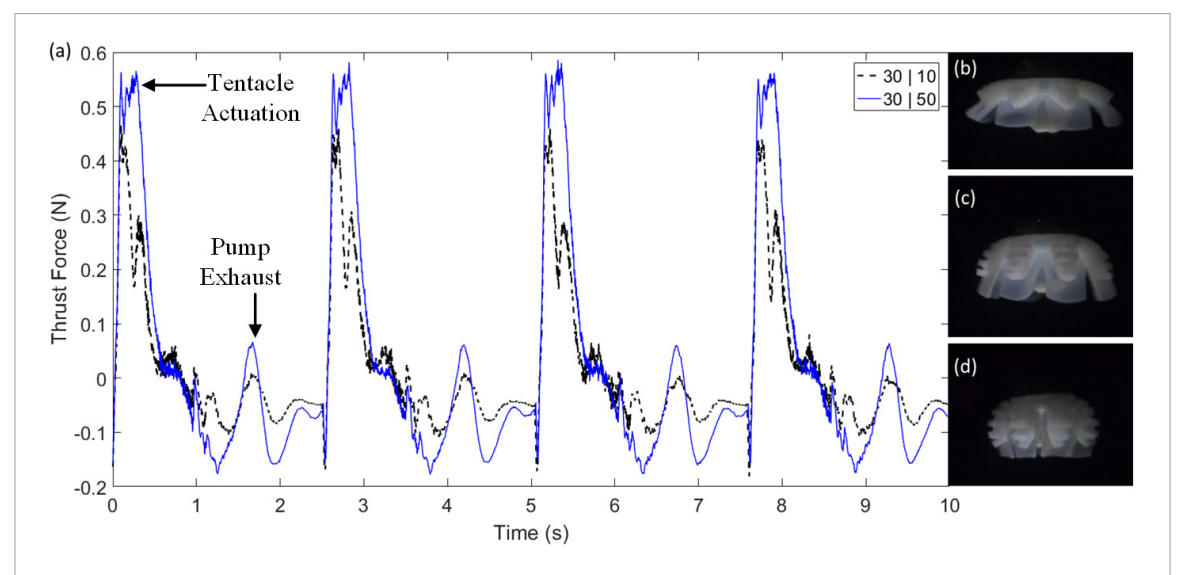


Figure 5. (a) Four representative cycles of load cell force measurement from two different jellyfish with tentacle-flap Shore hardness compositions of 30-10 and 30-50. The increase in thrust force due to the actuation stroke of the tentacles as well as the pump generated from the pump exhaust is labeled. These effects are coupled. The actuation frequency was 0.4 Hz with a full stroke actuation amplitude, starting from fully open to fully closed similar the sequence in (b)–(d).

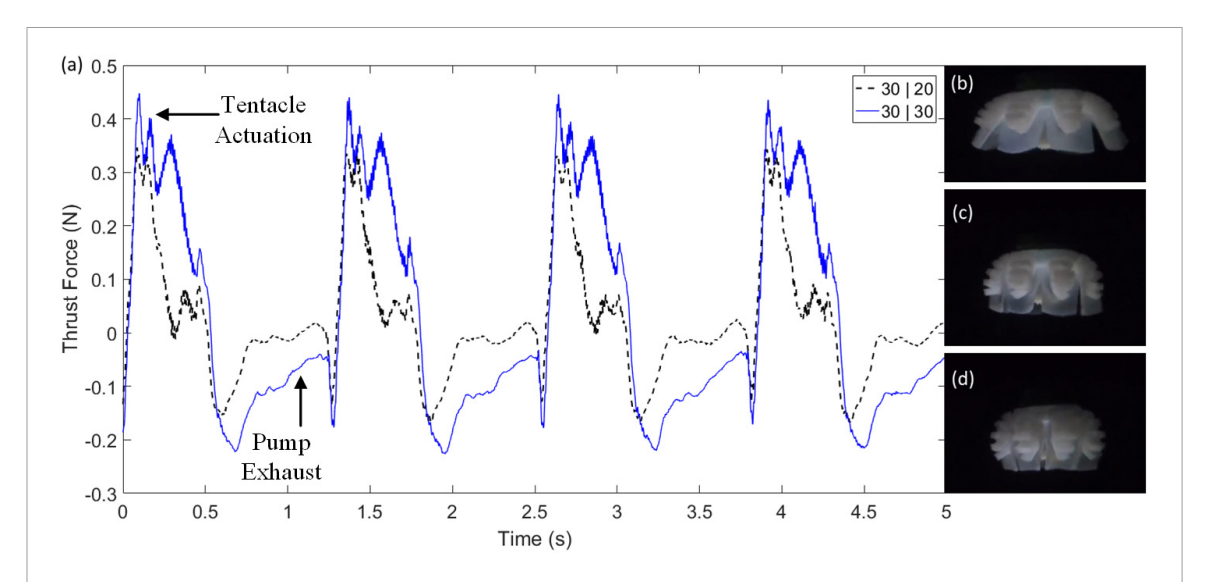


Figure 6. (a) Four representative cycles of load cell force measurement from two different jellyfish with tentacle-flap Shore hardness compositions of 30–20 and 30–30. The increase in thrust force due to the actuation stroke of the tentacles as well as the pump generated from the pump exhaust is labeled. These effects are coupled. The actuation frequency was 0.8 Hz with a half stroke actuation amplitude, starting from halfway contracted to fully flexed, similar the sequence in (b)–(d).

For example, 30–10 refers to a jellyfish fabricated using soft soft hydraulic actuators with a Shore hardness of 30 that were bonded to a silicon rubber flap with a Shore hardness of 10. Thirty actuation cycles of load cell data were collected for analysis with each composition of five material Shores, ten actuation frequencies, and two stroke amplitudes. A three-factor analysis of variance (ANOVA) was performed on these data to determine the statistical significance that the material Shore hardness, actuation stroke amplitude, and actuation frequency had upon the measured force with the 'anovan' function in MATLAB.

To measure the force produced during the actuation strokes of the jellyfish robot, a Futek 2 lb JR S-Beam load cell was used with a Futek CSG110 Strain

Gauge Universal Amplifier, both of which were powered by a BK Precision 1672 power supply. The load cell was connected to the center of the jellyfish electronics canister lid via a steel rod parallel to gravity. The amplified load cell signal was sampled at 1 kHz in Simulink using a National Instruments PCI-6229 data acquisition card and the real-time Windows target kernel. The load cell was tared and the calibration was verified at the beginning of each experiment to determine the amount of force generated by the actuation strokes without any impact from buoyancy. To maximize the jellyfish thrust force in this three factor study, both impeller pumps were driven by identical square waves to produce 100% pulse width modulation (PWM) duty cycles during each actuation stroke.

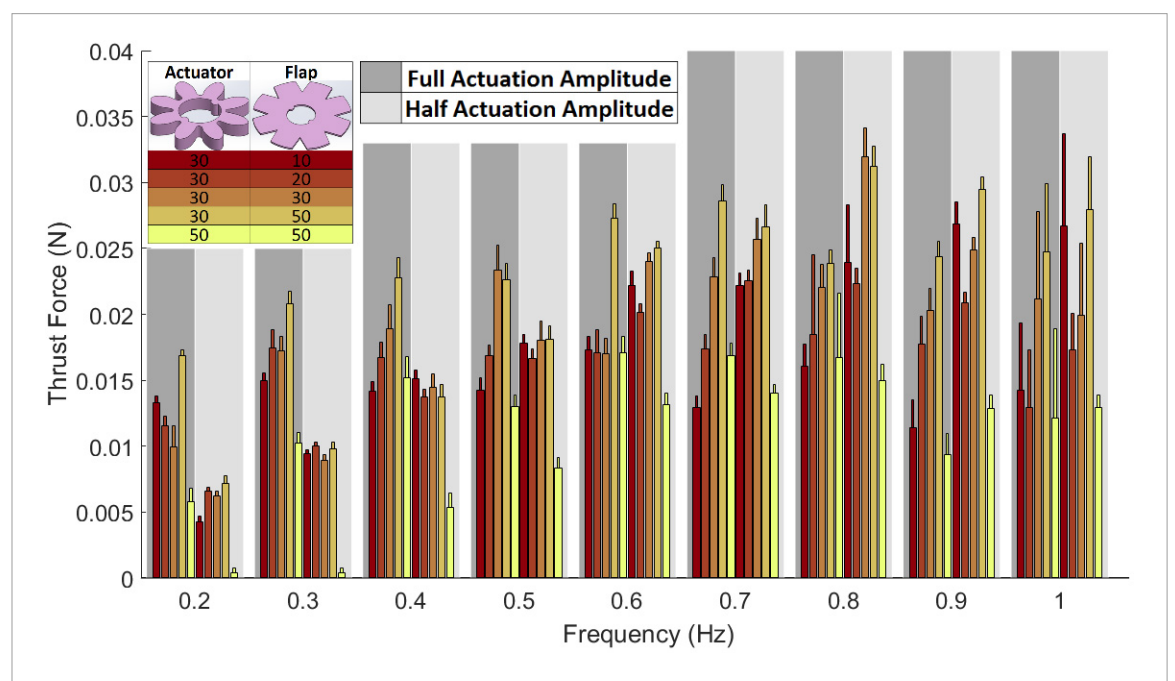


Figure 7. Mean force measurements from five different jellyfish actuated over a frequency range from 0.2 Hz to 1 Hz, each with two different actuation stroke amplitudes. Jellyfish with tentacle-flap Shore hardness compositions of 30–30 and 30–50 performed the best. The full stroke amplitude of actuation produced larger forces with lower actuation frequencies whereas the half stroke actuation stroke produced the largest force overall at a frequency of 0.8 Hz.

4. Results

4.1. Tentacle posture control revealed jellyfish natural frequency

Sinusoidal tracking data can be seen in figure 4(b) where both sides of the jellyfish were driven by a 0.1 Hz sine wave. The tri-level step response of the jellyfish robot revealed nearly undamped system dynamics (figure 4(c)) during the first and second portions of the step input before fully saturating due to the valve-free design of the hydraulic network actuation system. This occurred because the impeller pumps were driven until the error was reduced to be within the pump deadband voltages, which caused a cessation of water inflow to the tentacles, whose inherent elasticity then caused the water to be squeezed back into the environment. This caused the tentacles to partially return to their relaxed state until their error signals subsequently increased above the pumps' deadbands, driving the pumps again in a repetitive, oscillatory manner.

It was observed that the frequency of oscillation for both sets of four tentacles was approximately 0.7 Hz. To determine this, the average period of all cycles of oscillation for both sets of pump-tentacle actuator networks was measured. The inverse of this average period produced the natural frequency, which is approximately 0.7 Hz for both sets of tentacle-pump actuation systems. This soft robotic jellyfish is not a second order system, but the dominant poles of the system have a frequency of oscillation of approximately 0.7 Hz. Since there is very little decay in the amplitude of the oscillations in the illustrative step response data (figure 4(c)), it is reasonable to approximate the impact of higher order dynamics (for example, inducting the second order dynamics).

ance from the pumps) as having negligible impact on the step response. Thus, the frequency of oscillation serves as a reasonable estimate of the natural frequency of the dominant undamped poles of the system [40]. Adequate position tracking performance of this nearly undamped system was obtained provided that the frequency of the desired input was well below the natural frequency of the system (figure 4(b)).

4.2. Thrust force measurements

The load cell data was consistent over the 30 actuation cycles measured with each combination of the three independent variables (frequency, amplitude, material). Illustrative data from four actuation cycles with two different actuator-flap material Shore compositions of 30–10 and 30–50 with a full-amplitude actuation stroke at 0.4 Hz frequency are shown in figure 5(a). Another plot showing representative data from two jellyfish with 30–20 and 30–30 actuator-flap material Shore compositions with a half-stroke actuation amplitude at a 0.8 Hz frequency is shown in figure 6(a).

There are two sources of thrust generation with this soft robotic jellyfish due to the open circuit of water flow. First, the tentacles when they are actuated, and second, the exhaust of water into the environment through the pumps when the tentacles return to their relaxed state. These two sources of thrust generation are directly coupled. Positive thrust generated by the exhaust of the pumps occurs due to the elasticity of the silicon rubber material constricting the water out of the tentacle actuators, through the impeller pumps, and into the environment. Hence, as the tentacles return to their relaxed, uninflated state (reducing thrust force),

water is simultaneously exhausted into the environment through the pumps, producing positive thrust. This generated a characteristic increase in thrust force as the tentacles returned to their passive posture. While these effects are coupled, the portions of the actuation cycle where the tentacles or pumps dominated the generated thrust force are labeled in figures 5 and 6.

Thrust force averages and standard deviations from all tests were plotted in figure 7. Data from 0.1 Hz is not presented because it consistently produced minimal or negative mean thrust. One observation was that the jellyfish actuator-flap material Shore hardness compositions of 30–30 and 30–50 consistently outperformed all other material compositions. The largest thrust forces were produced with a half-stroke actuation amplitude at a frequency of 0.8 Hz.

The ANOVA showed that not only was each of the three independent variables (material Shore, actuation frequency, actuation amplitude) significant, but also the interactions between material-frequency, material-amplitude, and frequency-amplitude were significant (p < 0.05). The three-factor interaction of material-frequency-amplitude also proved significant (p < 0.05).

A reasonable explanation for the interaction between actuation stroke amplitude and frequency can be seen, for example, with the jellyfish robot with a material Shore hardness composition of 30–50. When this robot was driven with a full actuation stroke amplitude, lower actuation frequencies from 0.2 Hz to 0.7 Hz produced larger forces than the corresponding half stroke amplitude experiments. However, the higher actuation frequencies (0.8–1 Hz) produced larger thrust forces when operating at a half actuation stroke amplitude (figure 7). A similar pattern can be seen with the jellyfish robot with a material Shore hardness composition of 30–30.

The interaction between material Shore hardness and actuation frequency can be seen since the pattern of thrust forces produced by the five different jellyfish robots varies substantially across frequencies.

Likewise, the interaction between the two independent variables of actuation stroke amplitude and jellyfish body Shore hardness can be also be seen. For example, at a frequency of 0.2 Hz, the jellyfish robot with the material Shore hardness composition of 50–50 had a much lower mean thrust force with a half amplitude stroke than the jellyfish with a Shore hardness composition of 30–10 with a full amplitude actuation stroke. However, the 50–50 jellyfish had a higher thrust force with a full amplitude stroke than the 30–10 jellyfish with a half amplitude actuation stroke.

This two-factor interaction effect gradually shifted as the third factor (frequency of actuation) was incremented, until a nearly opposite situation was true at high frequencies of actuation. For example, at 0.9 and 1 Hz actuation frequencies, the 50–50 robot with a full amplitude actuation stroke has a mean thrust force approximately half that of the 30–10 robot with a half

amplitude actuation stroke. On the other hand, the 50–50 robot with a half amplitude stroke had nearly the same force generated as the 30–10 robot with a full amplitude actuation stroke. This gradual shift in behavior between the interaction of these two independent variables (actuation stroke amplitude and jellyfish material composition) as the third independent variable (frequency) was incremented illustrates the interaction of the three independent variables and the complexity of the design and control problem.

5. Discussion

5.1. Soft robotic jellyfish design observations

It has been observed that the frequency of live jellyfish body contractions impacts their swimming speed [21], and that the frequency of robotic fish actuation impacts thrust [39]. The mean thrust data in this paper show a general trend where the measured force increased with actuation frequency until it peaked around 0.7 Hz (full actuation stroke amplitude, 30–50 Shore hardness composition) or 0.8 Hz (half actuation stroke amplitude, 30–30 Shore hardness composition) before it attenuated at higher frequencies (figure 7). In the case of the soft robotic jellyfish, it was observed that the natural frequency was approximately 0.7 Hz (figure 4(c)). Also the peak of the thrust force occurs close to 0.7 Hz (figure 7). The proximity of peak thrust forces to the natural frequency of the jellyfish suggests that the soft robotic jellyfish could improve its swimming performance if the driving frequency is close to its natural frequency.

This compares well with the jellyfish robot that had rigid six-bar linkage actuated tentacles that exhibited a maximum swimming speed at an actuation frequency of 0.95 Hz [23]. For rigid propulsors in inertial dominated flows, thrust force is expected to scale by the square of the driving frequency of the thrusting surface or fin and to scale linearly with the amplitude of oscillation [13]. However, for highly flexible propulsors, fluid-structure interactions are likely to generate somewhat different fin kinematics affecting thrust generation. But it has been shown that flexible propulsors can improve their propulsive efficiency when the driving frequency is close to the natural frequency compared to rigid propulsors [10, 41, 42]. The improvement in performance results from the changes in the kinematics and the interaction of the flexible propulsor with the surrounding fluid and its wake. However, a thorough understanding of this relationship is still an open area of research for soft robotic propulsors [10, 41, 42].

Results in this paper have also shown that the actuator material Shore hardness is an important parameter in the complex underwater soft robot design space. It is likely that the low Shore hardness compositions of soft robotic jellyfish in this paper (30–10 and 30–20) were too weak in comparison to the inertia and viscosity of the fluid (water). On the other hand, the highest

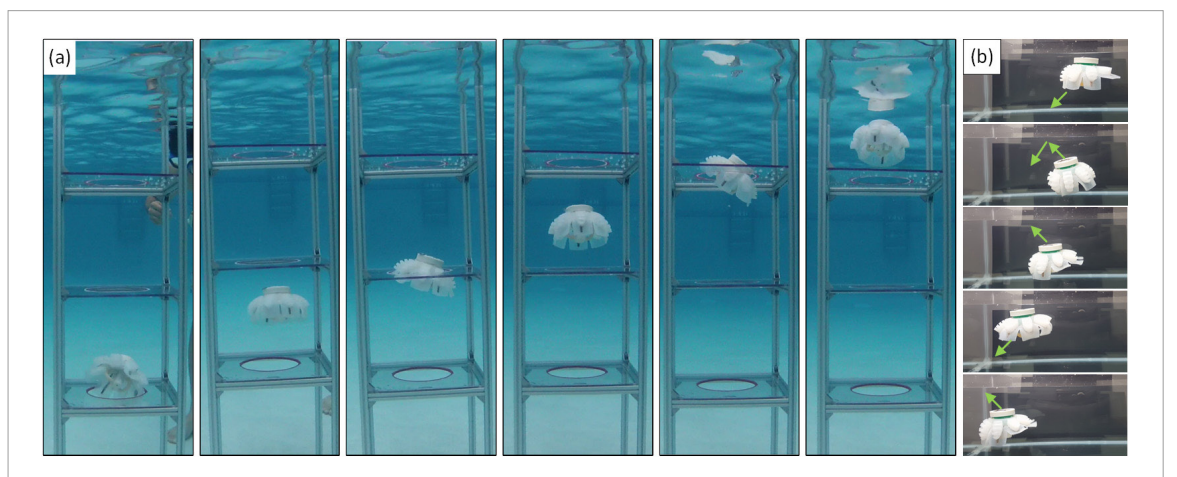


Figure 8. (a) The robot was able to swim through three orifices that are smaller than the nominal diameter of the jellyfish. See also the supplementary video. (b) By actuating opposite sides of the robot at different times, the jellyfish was able to steer.

Shore hardness jellyfish material composition (50–50) was likely too stiff to be rapidly and fully inflated by the pumps, which is the most probable explanation as to why the 30–30 and 30–50 Shore hardness compositions consistently outperformed the lower and higher material Shore compositions.

5.2. Flexible jellyfish body enabled swimming through orifices

One advantage of soft robots is the potential to squeeze through narrow conduits. The ability of the robotic jellyfish to swim through apertures more narrow than its nominal diameter was tested first in an aquarium with a circular orifice cut within a plexiglass plate. The circular orifice had a diameter of 152 mm, to offer a mild challenge to swim through. The jellyfish with a shore hardness composition of 30–30 was used in this experiment, with a full stroke actuation amplitude and an actuation frequency of 0.4 Hz. The jellyfish was submerged in the aquarium underneath the plexiglass plate and allowed to swim vertically upward through the orifice. The jellyfish robot collided with the edge of the orifice, but was able to generate enough thrust as it contracted to pass through the orifice (see supplementary video (stacks.iop.org/BB/13/064001/ mmedia)).

Another set of swim-through experiments were performed with a three story square structure that was submerged in a swimming pool. A square plate with a circular hole was placed on each of the three levels of the structure. The circular holes were 160 mm in diameter, which is smaller than the 210 mm diameter of the jellyfish to pose a moderate challenge to vertically swim through. Because the horizontal motion of the jellyfish was not directly controlled in this experiment, it would enter the apertures off-center and become temporarily stuck. However, after several contraction cycles of the actuators, it was able to wriggle through the openings (figure 8(a), video supplement). This experiment was performed with a jellyfish robot with a Shore hardness composition of 30–50, which was pro-

grammed to repeatedly actuate both sets of hydraulic network tentacle actuators simultaneously with a half stroke amplitude and a frequency of 0.7 Hz.

In the future, a suite of environmental sensors should be integrated into the soft robotic jellyfish control algorithm to enable the performance of these types of swim-through maneuvers with high success rates. This environmental information should be coupled with a navigational algorithm that is reliant upon the IMU to properly orient and align the jellyfish with the orifice. While the feasibility of swim-through maneuvers has been presently demonstrated, the lack of such environmental sensors on the current jellyfish prototype are not conducive to robustly perform swimthrough maneuvers in an unstructured environment. The use of sonar sensors and/or video imaging would enable the jellyfish to locate orifices and determine whether or not it is feasible and useful to perform the swim-through.

5.3. Jellyfish steering and open water experiments

Live jellyfish can turn via an asymmetric contraction of the bell [20]. The ability of the soft robotic jellyfish to steer from side to side in an aquarium was verified by temporally offsetting the actuation strokes of each side of the jellyfish, producing asymmetric tentacle motion profiles. By alternately actuating the opposing sides of the jellyfish at different times, laterally directed components of thrust were generated producing motion from right to left (figure 8(b)).

Open water tests were conducted in three locations in the Atlantic Ocean off the coast of Florida, USA. The first testing site was a buried wreck approximately 350 m off the coast of Delray Beach (figures 1(a) and (b)). The second testing site was approximately 300 m offshore at the EroJacks artificial reef in Dania Beach (figure 1(d)). The third testing site was roughly 200 m off the coast of Boca Raton at Boca Artificial Reef (figure 1(e)). The increased buoyancy of the saltwater relative to the freshwater pool and aquarium experiments necessitated additional trim weights to provide a negative net jelly-



Figure 9. Photo sequence of the soft robotic jellyfish traveling laterally across the reef by actuating only one set of four pneumatic actuator tentacles. See also video supplement.

fish buoyancy. The jellyfish were submerged to a maximum depth of approximately 5 m and allowed to swim vertically to the surface to demonstrate their potential in open water (figures 1 and 4(a)). The ability to swim laterally in the ocean by actuating four pneumatic actuator tentacles on only one side of the jellyfish robot body was also tested (figure 9, supplemental video).

The open water experiments in the ocean, in addition to the orifice swim-through and steering experiments (figures 8 and 9) suggest that this jellyfish robot prototype has the potential to nondestructively monitor fragile ecosystems. It is envisioned that the robotic jellyfish would perform well in a drift-dive situation where they could be submerged in one location and allowed to drift to another location in the ocean current with nominal maneuverability within the water column if features of interest were detected (figure 9).

6. Conclusion

Five unique soft robotic jellyfish were constructed with hydraulic network actuators. Results showed that the material composition of the actuators significantly impacted the measured force produced by the jellyfish, as did the actuation frequency and stroke amplitude. The greatest forces were measured with a half-stroke amplitude at 0.8 Hz and a tentacle actuator-flap material Shore hardness composition of

30–30. The jellyfish was able to swim through orifices more narrow than the nominal diameter of the robot and demonstrated the ability to swim directionally by temporally offsetting tentacle actuation strokes on opposing sides of the robot. The jellyfish robots were tested in the ocean and have the potential to monitor and explore delicate ecosystems without inadvertently damaging them.

ORCID iDs

Oscar Curet https://orcid.org/0000-0002-3202-6841

Erik D Engeberg https://orcid.org/0000-0002-2340-1881

References

- [1] Galloway K C et al 2016 Soft robotic grippers for biological sampling on deep reefs Soft Robot. 3 23–33
- [2] Majidi C 2014 Soft robotics: a perspective—current trends and prospects for the future *Soft Robot*. 15–11
- [3] Faudzi A A M, Razif M R M, Nordin N A M, Natarajan E and Yaakob O 2014 A review on development of robotic fish J. Transp. Syst. Eng. 1 12–22
- [4] Raj A and Thakur A 2016 Fish-inspired robots: design, sensing, actuation, and autonomy—a review of research *Bioinspir*. *Biomimet*. 11 031001
- [5] Marchese A D, Onal C D and Rus D 2014 Autonomous soft robotic fish capable of escape maneuvers using fluidic elastomer actuators Soft Robot. 175–87
- [6] Calisti M et al 2011 An octopus-bioinspired solution to movement and manipulation for soft robots Bioinspir. Biomimet. 6 036002
- [7] Cianchetti M, Calisti M, Margheri L, Kuba M and Laschi C 2015 Bioinspired locomotion and grasping in water: the soft eight-arm OCTOPUS robot *Bioinspir*. *Biomimet*. 10 035003
- [8] Laschi C, Cianchetti M, Mazzolai B, Margheri L, Follador M and Dario P 2012 Soft robot arm inspired by the octopus Adv. Robot. 26 709–27
- [9] Kim H-J, Song S-H and Ahn S-H 2012 A turtle-like swimming robot using a smart soft composite (SSC) structure Smart Mater. Struct. 22 014007
- [10] Liu H, Taylor B and Curet O M 2017 Fin Ray Stiffness and Fin Morphology Control Ribbon-Fin-Based Propulsion Soft Robot. 4 103–16
- [11] Suzumori K, Endo S, Kanda T, Kato N and Suzuki H 2007 A bending pneumatic rubber actuator realizing soft-bodied manta swimming robot 2007 IEEE Int. Conf. on Robotics and Automation pp 4975–80
- [12] Villanueva A, Smith C and Priya S 2011 A biomimetic robotic jellyfish (robojelly) actuated by shape memory alloy composite actuators *Bioinspir. Biomimet.* 6 036004
- [13] Bale R, Hao M, Bhalla A P S and Patankar N A 2014 Energy efficiency and allometry of movement of swimming and flying animals *Proc. Natl Acad. Sci.* 111 7517–21
- [14] Gemmell B J *et al* 2013 Passive energy recapture in jellyfish contributes to propulsive advantage over other metazoans *Proc. Natl Acad. Sci.* **110** 17904–9
- [15] Dabiri J O, Colin S P, Costello J H and Gharib M 2005 Flow patterns generated by oblate medusan jellyfish: field measurements and laboratory analyses J. Exp. Biol. 208 1257– 65
- [16] Gemmell B J, Troolin D R, Costello J H, Colin S P and Satterlie R A 2015 Control of vortex rings for manoeuvrability J. R. Soc. Interface 12 20150389
- [17] McHenry M J and Jed J 2003 The ontogenetic scaling of hydrodynamics and swimming performance in jellyfish (Aurelia aurita) *J. Exp. Biol.* 206 4125–37

- [18] Colin S P and Costello J H 2002 Morphology, swimming performance and propulsive mode of six co-occurring hydromedusae J. Exp. Biol. 205 427–37
- [19] Gemmell B J, Colin S P, Costello J H and Dabiri J O 2015 Suction-based propulsion as a basis for efficient animal swimming Nat. Commun. 6 8790
- [20] Shanks A L and Graham W M 1987 Orientated swimming in the jellyfish Stomolopus meleagris L. Agassiz (Scyphozoan: Rhizostomida) J. Exp. Mar. Biol. Ecol. 108 159–69
- [21] Petie R, Garm A and Nilsson D-E 2013 Contrast and rate of light intensity decrease control directional swimming in the box jellyfish tripedalia cystophora (Cnidaria, Cubomedusae) *Hydrobiologia* 703 69–77
- [22] Albert D J 2008 Adaptive behaviours of the jellyfish Aurelia labiata in Roscoe Bay on the west coast of Canada J. Sea Res. 59 198–201
- [23] Yu J, Xiao J, Li X and Wang W 2016 Towards a miniature selfpropelled jellyfish-like swimming robot *Int. J. Adv. Robot. Syst.* 13 1729881416666796
- [24] Villanueva A, Priya S, Anna C and Smith C 2010 Robojelly bell kinematics and resistance feedback control 2010 IEEE Int. Conf. on Robotics and Biomimetics (ROBIO) pp 1124–9
- [25] Tadesse Y, Villanueva A, Haines C, Novitski D, Baughman R and Priya S 2012 Hydrogen-fuel-powered bell segments of biomimetic jellyfish Smart Mater. Struct. 21 045013
- [26] Najem J, Sarles S A, Akle B and Leo D J 2012 Biomimetic jellyfish-inspired underwater vehicle actuated by ionic polymer metal composite actuators Smart Mater. Struct. 21 094026
- [27] Yeom S-W and Oh I-K 2009 A biomimetic jellyfish robot based on ionic polymer metal composite actuators Smart Mater. Struct. 18 085002
- [28] Godaba H, Li J, Wang Y and Zhu J 2016 A soft jellyfish robot driven by a dielectric elastomer actuator *IEEE Robot. Automat.* Lett. 1 624–31
- [29] Ko Y et al 2012 A jellyfish-like swimming mini-robot actuated by an electromagnetic actuation system Smart Mater. Struct. 21 057001

- [30] Marut K, Stewart C, Michael T, Villanueva A and Priya S 2013 A jellyfish-inspired jet propulsion robot actuated by an iris mechanism *Smart Mater. Struct.* 22 094021
- [31] Nir S, Ruchaevski I, Shraga S, Shteinberg T and Moshe B B 2012 A jellyfish-like robot for mimicking jet propulsion 2012 IEEE 27th Convention of Electrical & Electronics Engineers in Israel (IEEEI) pp 1–5
- [32] Nawroth J C et al 2012 A tissue-engineered jellyfish with biomimetic propulsion *Nat. Biotechnol.* **30** 792–7
- [33] Mosadegh B et al 2014 Pneumatic networks for soft robotics that actuate rapidly Adv. Funct. Mater. 24 2163–70
- [34] Frame J, Curet O and Engeberg E 2016 Free-swimming soft robotic jellyfish *Florida Conf. on Recent Advances in Robotics* (*Miami*) pp 100–5
- [35] Lopez N and Engeberg E D 2017 Soft robotic jellyfish steering control Florida Conf. on Recent Advances in Robotics (Boca Raton)
- [36] Polygerinos P et al 2013 Towards a soft pneumatic glove for hand rehabilitation 2013 IEEE/RSJ Int. Conf. on Intelligent Robots and Systems (IROS) pp 1512–7
- [37] Hoover A, Griffith B and Miller L 2017 Quantifying performance in the medusan mechanospace with an actively swimming three-dimensional jellyfish model *J. Fluid Mech.* 813 1112–55
- [38] Bajcar T, Malacic V, Malej A and Širok B 2009 Kinematic properties of the jellyfish Aurelia sp Hydrobiologia 616 279– 89
- [39] Nguyen P L, Lee B R and Ahn K K 2016 Thrust and swimming speed analysis of fish robot with non-uniform flexible tail J. Bion. Eng. 13 73–83
- [40] Ogata K 2010 Modern Control Engineering 5th edn (Upper Saddle River, NJ: Pearson)
- [41] Alben S 2008 Optimal flexibility of a flapping appendage in an inviscid fluid *J. Fluid Mech.* 614 355–80
- [42] Dewey P A, Boschitsch B M, Moored K W, Stone H A and Smits A J 2013 Scaling laws for the thrust production of flexible pitching panels *J. Fluid Mech.* **732** 29–46